Supplementary Information (SI)

A Facile Spin-Cast Route for Cation Exchange of Multilayer Perpendicularly-Aligned Nanorod Assemblies

Dervla Kelly[abc], Ajay Singh[abc], Christopher A. Barrett[ab⊥], Catriona O'Sullivan[ab], Claudia Coughlan[ab], Fathima R. Laffir[a], Colm O'Dwyer[ad] and Kevin M. Ryan*[abc]

[a]Materials and Surface Science Institute, Department of Chemical and Environmental Sciences, University of Limerick, Limerick, Ireland.

[b]Department of Chemical and Environmental Sciences

[c]SFI-Strategic Research Cluster in Solar Energy Research, University of Limerick, Limerick, Ireland.

[d]Department of Physics, University of Limerick, Ireland.

[⊥]Department of Chemistry, University of Georgia, Athens, 30602, USA (Current Address)

E-mail: kevin.m.ryan@ul.ie; Tel: +353 61213167

Experimental Data:

Spin exchange Process

The assembly of the nanorods was undertaken by two methods – electrophoretic deposition or drop cast methods. The electrophoretic deposition method involves the utilisation of a conducting substrate, such as ITO or silicon, which was clamped to the negative electrode and a DC field of 200V was applied, resulting in conformal deposition of nanorods on the substrate. Layers of nanorods were formed by varying the concentration of the rods in solution and the time over which the deposition was allowed to take place. Self-assembly of the nanorods involved exploiting the dipole forces in the slow evaporation of a droplet. Following this, the nanorods were spin exchanged. This involved covering the substrate with a layer of either $AgNO_3$ in methanol or tetrakis(acetonitrile)copper(I) hexafluorophosphate in methanol and spinning the substrate at 500 rpm for 50 seconds in the spin coater. When this methodology was applied to TEM grids, 20µL of the respective solution was placed on the grid which was spun at 100 rpm for 30 seconds. The centrifugal forces applied here allowed

the nanorod layers to be evenly cation exchanged due to the conformal distribution of the solution throughout the layer of nanorods on the substrate while removing any of the excess material (Cadmium, surfactants).

Synthesis of CdS and CdSe nanorods

Cadmium sulfide (CdS), cadmium selenide (CdSe) nanorods were prepared using standard air free conditions using standard schenlk line techniques and dispersed in toluene before use.

CdS Synthesis

In a typical synthesis, 0.20g of CdO, 1.07 g of ODPA and 2.74 g of TOPO were loaded into a 25 ml three-neck round bottom flask, fitted with a reflux condenser and a rubber septum. The contents of the flask were heated to 100 °C under Argon gas until the reactants dissolve. At this point, a brown solution is evident in the flask. The flask is then evacuated at 100°C for one hour to remove any excess moisture. The mixture is then heated to 300°C under Ar-gas where the CdO completely dissolves and the solution becomes optically clear. The mixture is cooled to 100°C and further degassed for another 30 minutes. After this second degas, the apparatus is switched back to the argon line and the mixture was heated to 300°C. 0.8 g of sulphur stock solution (0.65 g of sulphur powder dissolved in 8.25 g of TOP) was injected into the flask. After injection, nanocrystals grew at 300°C for 30 minutes to reach desired size. The nanorods were washed to remove an excess surfactant by dispersing them in a 1:1 ratio of acetone to toluene followed by 60 s agitation and 120 s sonication. The solution was then centrifuged at 3000 rpm for 180 s and the sediment was decanted from the supernatant.

CdSe Synthesis

CdSe nanorods were also synthesised in a procedure similar to that of CdS nanorods. Briefly, CdO (0.20g), n-tetradecylphosphonic acid (TDPA,710mg), n-Hexylphosphonic acid (HPA,160g) and tri-n-octylphosphine oxide (TOPO, 3.00g) were loaded in 25 ml three-neck flask equipped with a condenser and a thermocouple adapter. The mixture is ramped to 120ºC under Ar atmosphere and then evacuated for 60 minutes. Following this, the solution is heated to 300ºC under Ar atmosphere so that CdO decomposed and gives an optical clear solution. Once an optical clear solution was achieved, 1.5g of Trioctylphosphine (TOP) was added to the mixture, and the temperature was further raised to 310ºC. Next, the stock solution of selenium (~500µl), which contains 73 mg of selenium in 416 mg of TOP, was

injected to the vigorously stirring Cd solution and the resulting particles were further allowed to grow for 5-10 min at 310ºC. The nanorod growth was terminated by removal of the heating mantle and at 80ºC, 2-4 ml of anhydrous toluene was added to the mixture to quench the reaction. The nanorods were purified by dissolution in toluene and precipitation from anhydrous isoproponal. They were cleaned three times with toluene and isoproponal mixture and redispersed in toluene for further measurements.

Assembly of Nanorods

The CdS and CdSe nanorods were aligned using electrophoresis and self-assembly methods. The electrophoretic deposition method involves a solution of the nanorods solvated in toluene or chloroform with copper electrodes immersed in the solution. A DC electric field of 200V was passed through the electrodes for 2 minutes and the nanorods electro-migrate and deposite on the negative electrode.

The self-assembly of both CdS and CdSe nanorods was undertaken by drop-casting the nanorod solution with an optimum nanorod concentration onto the substrate. It was then allowed to dry under a slow evaporation rate. The strict concentration dependence of the nanorod solution is necessary for perpendicular nanorod assembly where outside of a certain window, nanorods deposit randomly on the substrate.

Spin Exchange of Aligned Nanorods

Solutions of silver nitrate and tetrakis(acetonitrile)copper(I) hexafluorophosphate in methanol were prepared. Concentrations of the solutions were altered depending on the concentrations of nanorods on the substrate. For ITO, silicon and glass concentrations varied from 0.008 – 0.1g/5ml. Approximately 0.5ml of the solution was dropped onto the substrate, on the spin coater and the rpm was set to 500rpm for 50 seconds. For TEM grids, much smaller concentrations of the silver/copper cation solutions were utilised. One to two drops of the solution was placed on the TEM grids and the spin coater was set to 100rpm for 30seconds. It should be noted that excess copper and silver atoms are required for exchange to take place, as some of the solution was spun off during the spin exchange process.

Equipment Used

Powder X-Ray Diffraction (XRD) spectra were obtained with a Philips X'Pert PRO MPD (Multi-purpose X-ray Diffractometer) operating with Cu Ka radiation. Transmission electron microscopy (TEM) was performed using a JEOL 2011 TEM with an accelerating voltage of 200 kV with samples being on carbon-coated copper TEM grids. The SEM micrographs were acquired using high resolution scanning electron microscopy (Hitachi S-4800 HRSEM). X-ray Photoelectron Spectroscopy data were collected in a Kratos AXIS 165 spectrometer using monochromatic Al Kα radiation (hυ =1486.6 eV) and a fixed pass energy of 20 eV. The binding energies were referenced to C 1s at 284.8 eV.

TEM & ED images

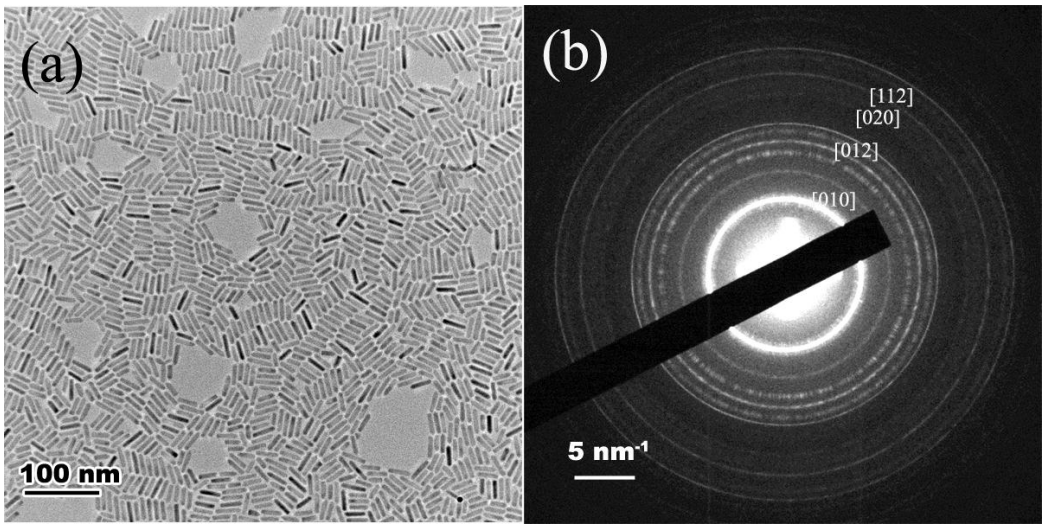

Fig. S1: (a) TEM image of CdS and (b) corresponding electron diffraction image.

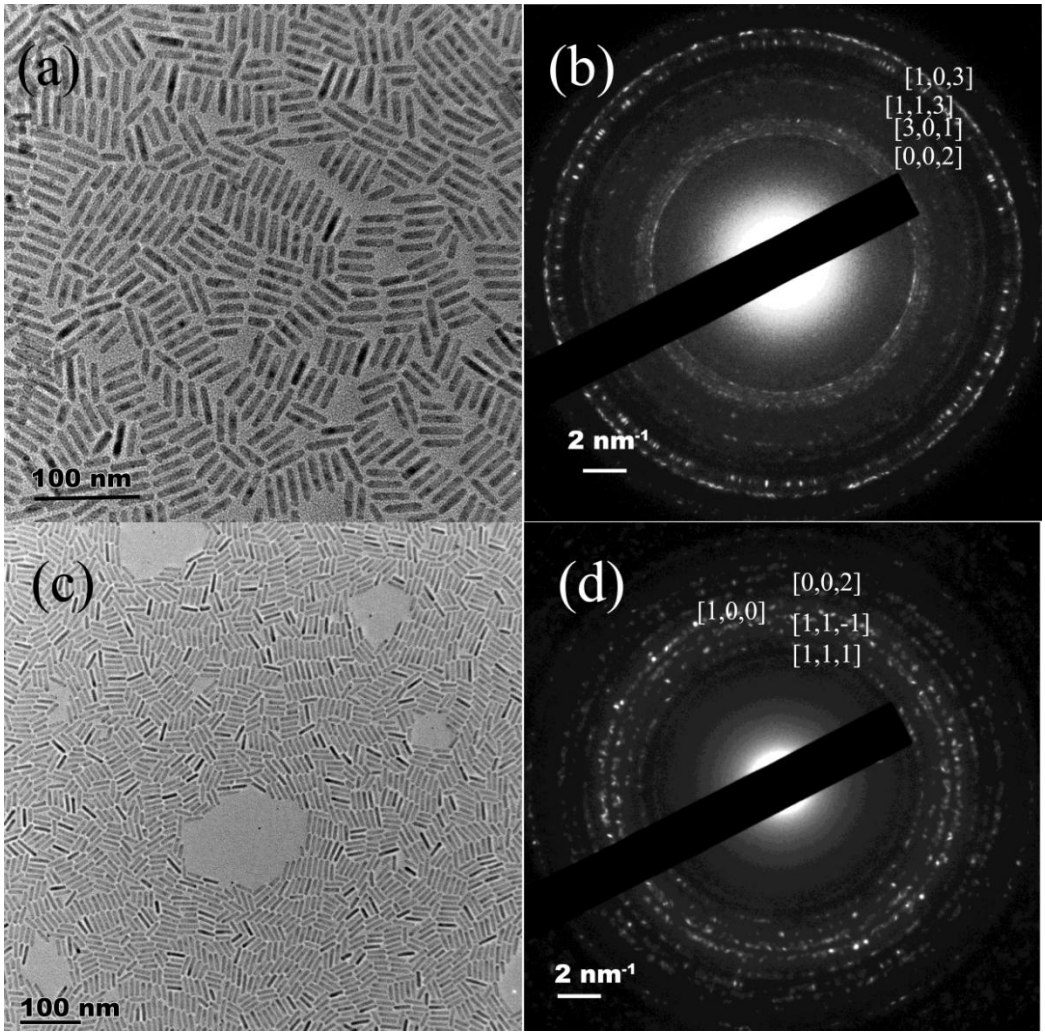

Fig. S2: Cu_7S_4 nanorods (b) electron diffraction of Cu_7S_4 and (c) Ag_2S nanorods and (d) electron diffraction of Ag_2S

SEM Images

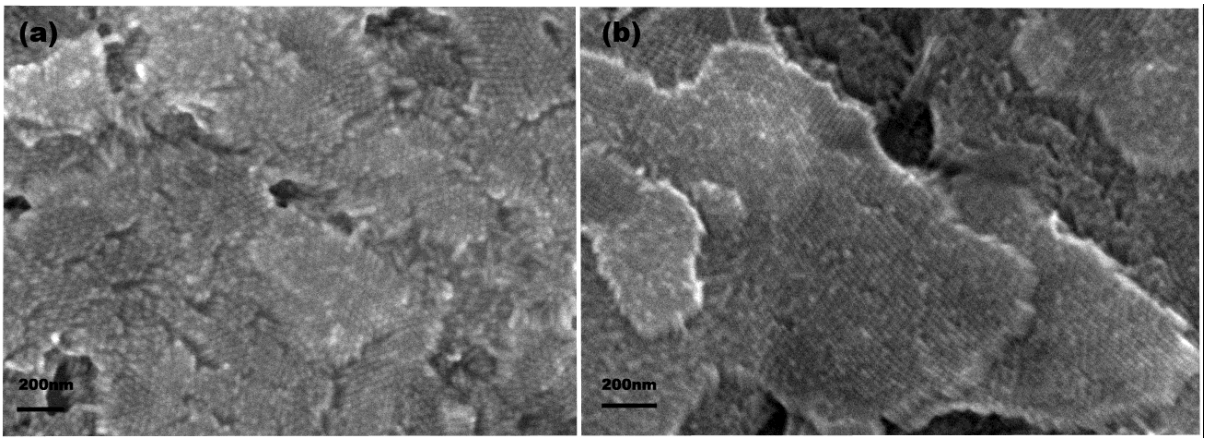

Fig S3: SEM images (a) & (b) display multilayer perpendicular assemblies of CdS nanorods

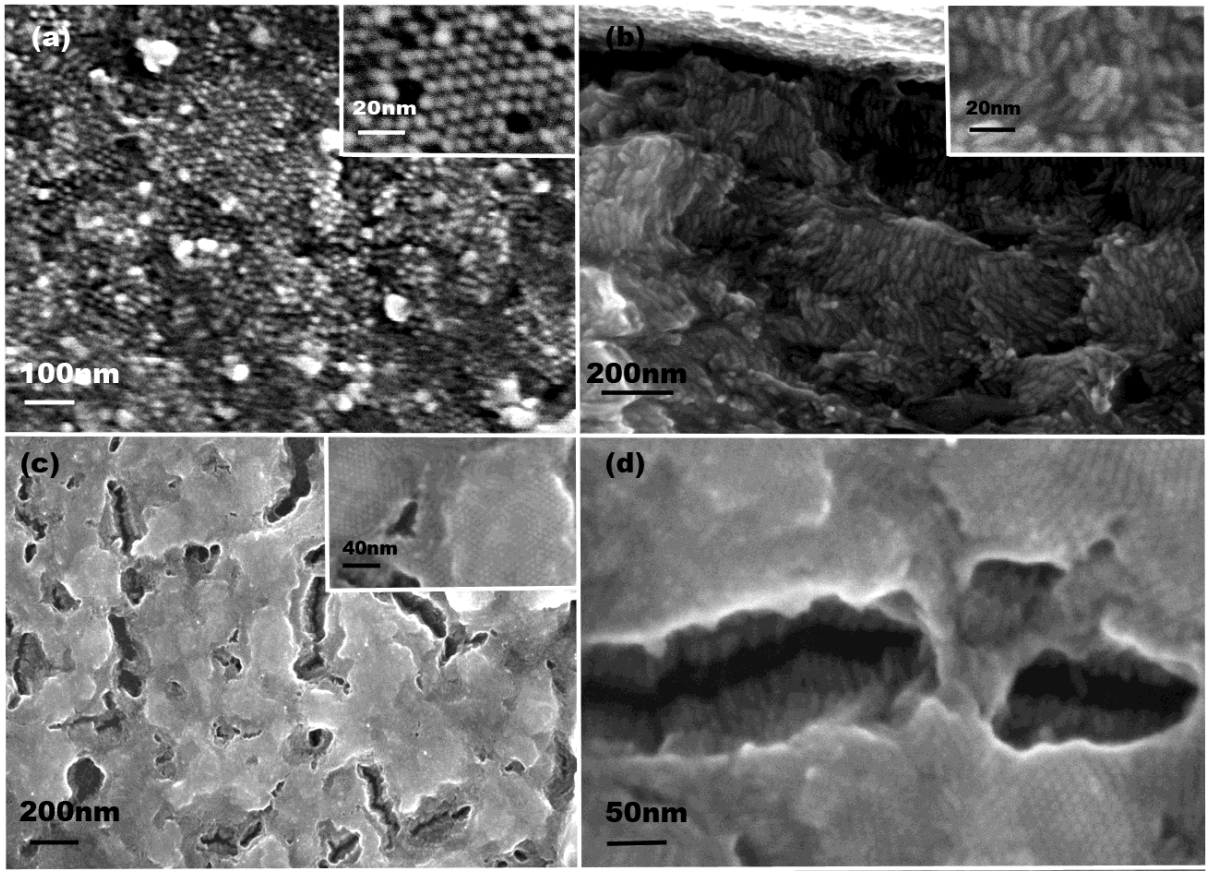

Fig S4: SEM images of (a) top down Ag_2S assembly with inset clearly showing tips of nanorods, (b) cross section Ag_2Se multilayer assembly with inset showing no shape change in the nanorods (c) top down Cu_7S_4 assembly over a large scale with inset showing a HRSEM image of assembly (d) side on view of Cu_7S_4 assembly with a view into the crack emphasising the multilayers of nanorods present within the assembly.

XRD Data

The XRD patterns in Fig. 3 (a) illustrate the complete conversion of CdS nanorods into Ag_2S and Cu_7S_4($Cu_{1.75}S$). The patterns confirmed the identity of the fully converted material as acanthite, Ag_2S, which has a monoclinic crystal structure. Peaks at 31.5, 34.4, 37.71, & 43.67 degrees 2θ are the main peaks which correspond to reflections (1,1,1), (1,2,0), (1,0,2) & (0,2 -3) respectively. Cu_7S_4, known as anilite, has an orthorhombic crystal structure. The main peaks at 26.5, 37,8, 46.3 & 48.77 degrees 2θ correspond to reflections (2,1,1), (3,0,2) (2,2,4) & (1,2,5). The XRD patterns in Fig. 3 (b) illustrate the full conversion of CdSe to Ag_2Se and Cu_3Se_2. For the sample exchanged to Ag_2Se, peaks at 24.0, 33.4, 36.9 and 45.0 degrees 2θ correspond to (1,1,0), (1,1,2),(0,1,3) and (0,3,2) reflections for the orthorhombic crystal

structure naumannite. Peaks at 25.0, 31.2, 44.7 and 51.3 degrees 2θ for the sample exchanged to Cu_3Se_2 correspond to the (0,1,1), (1,2,0), (1,3,0), and (0,2,2) reflections for the tetragonal crystalline structure umangite. There is no overlap when comparing the original CdSe diffractogram to the Ag_2Se and Cu_3Se_2 patterns which indicates that full cation exchange has taken place. The change in crystal structure is obvious due to the different x-ray crystalline diffraction patterns which were obtained.

Reitveld Analysis:

	XRD (wt. %)	R_{exp}	$R_{profile}$
Anilite Cu_7S_4	95	1.96	3.96
Chalcosite Cu_2S	5		

Table S1: Rietveld results for Cu_7S_4

	XRD (wt. %)	R_{exp}	$R_{profile}$
Umangite Cu_3Se_2	100	1.83	13.74
Copper (I) Selenide Cu_2Se	0		

Table S2: Reitveld results for Cu_3Se_2

Electrical measurements

Charge transport measurements were conducting using 2- and 4-probe measurements using a voltage-variable potentiostat and a Agilent 34401A Digital Multimeter. Current was measured using a home-built probe station and each device measured at a Peltier cell thermostated temperature of 295 K in a Faraday cage. Liquid metal contacts were made using In-Ga eutectic blown into a sphere from a gold metallized short borosilicate capillary tube ensuring identical contact areas. Measurements were made in van der Pauw[1] geometry for all types of nanorod assemblies and resistivity values were extracted from I-V curves in the high bias regime (series resistance) and also from 4-point probe measurements.

Current-voltage analysis of CdS, Ag_2S and Cu_7S_4 nanorod multilayer assemblies was analysed in the framework of both Schottky junction limited transport and also thermionic emission conduction. For Schottky contacts, the influence of barrier height lowering was not accounted for, but from comparison to recent results on single and layers of nanorods, and while it refines measurements of barrier heights etc., it does not influence the determination of the conduction mechanism.

For CdS, the I-V curve is indicative of Schottky junction transport. At low temperatures (room temperature) when the thermal activation of carriers is negligible, the current-voltage dependence suggests carriers tunnel onto the nanocrystal through a voltage-dependent contact barrier, i.e. a Schottky barrier. Similar electrical response from individual colloidal CdSe nanocrystals was also observed previously[2, 3]

The following expression gives the voltage-dependent tunneling current, I, through such a barrier

$$I = \Omega V \exp\left(-2\sqrt{\frac{4\pi^2 m^* \varepsilon_s}{h^2 N_D}}\left[\sqrt{(V+\varphi_B)\varphi_B} - V\alpha\right]\right)$$

where

$$\alpha = \cosh^{-1}\left(\sqrt{\frac{V+\varphi_B}{V}}\right)$$

and is the method used here to extract carrier concentration, barrier height and carrier mobility, since the electron and hole mobilities $\mu_{n,p} = (n,p)q/\rho$, where ρ is the resistivity determined from the high potential bias region. Φ_B is the barrier height, ε_s, N_D, and m^* are the semiconductor permittivity, doping concentration and effective mass of CdS, and Ω is the wave function coupling constant of the electrode to the nanorod. The fit also determines doping concentrations, N_D, by assuming the bulk CdS values for ε_s, and m^*.[4] For the Ag_2S assemblies, the symmetric response is best fitted with the thermionic emission model, in spite of being acquired at room temperature. We stress that although an asymmetric Schottky barrier can cause symmetry in the I-V response due to Fermi level changes with applied potential, all curves fitted best by Schottky theory did not follow trends associated with thermionic emission, which Ag_2S as a nanorod assembly does. Considering the typical behavior at bulk Au-Ag_2S interfaces, and the contact barriers observed during the low (room) temperature analysis, our devices consist of a rectifying junction at the Au contact. For a particular bias polarity, the higher potential side limits the total current across the device. Indeed, a high temperature conduction mechanism of thermionic emission over a reverse-biased Schottky diode fits the data very well and values were extracted from the current-voltage dependence

$$I = AA^{**}T^2 \exp\left(\frac{-q\varphi_B}{kT}\right)$$

and the electric field across the junction

$$E = \sqrt{\frac{2qN_D}{\varepsilon_s}\left(V + \varphi_{Bi} - \frac{kT}{q}\right)}$$

where A is the contact area, A^{**} is the effective Richardson constant, Φ_B is the ideal barrier height in the absence of an image force lowering (which is negligible in this case), E is the electric field, Φ_{Bi} is the built-in potential, ε_s and N_D are the semiconductor permittivity and doping concentration of Ag_2S.

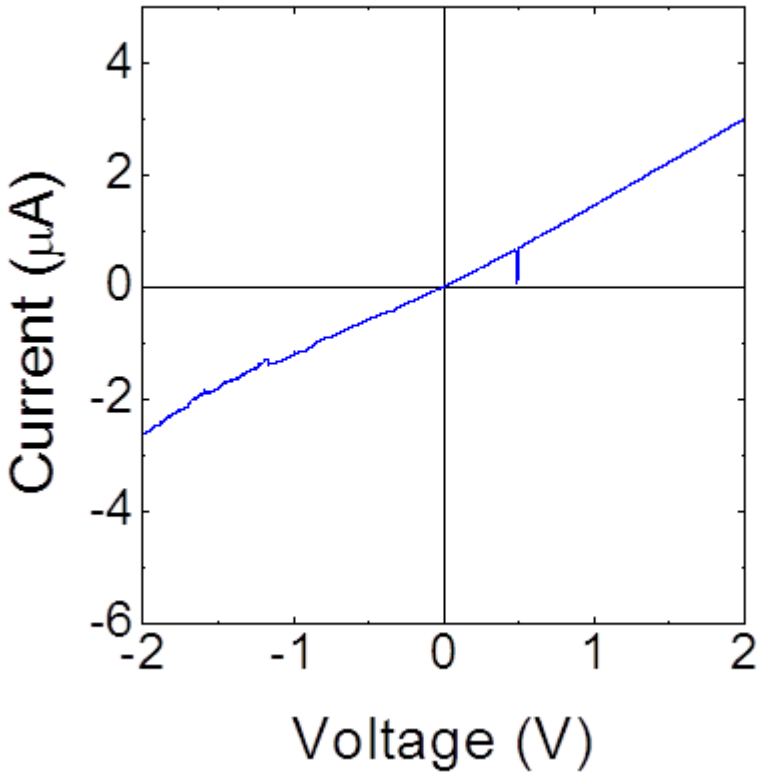

Fig. S5 Electrical measurements through spin exchanged Ag_2S as a thin deposit after sintering, exhibiting an ohmic response. The nanorod assembly was sintered to coalesce grains and removed organic contaminants from the surfactant employed to synthesize the nanorods and influence their assembly initially.

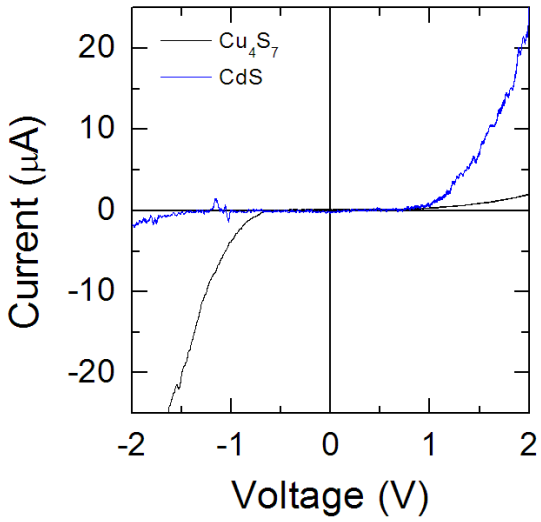

Fig. S6 Current-voltage curves for CdS and cation exchanged Cu_7S_4 nanorod assemblies showing n-type and p-type conduction, respectively

1. L. Van der Pauw, *Rep*, 1958, 13, 1.
2. M. S. Gudiksen, K. N. Maher, L. Ouyang and H. Park, *Nano Lett.*, 2005, 5, 2257-2261.
3. H. Steinberg, Y. Lilach, A. Salant, O. Wolf, A. Faust, O. Millo and U. Banin, *Nano Lett.*, 2009, 9, 3671-3675.
4. S. M. Sze and K. K. Ng, *Physics of semiconductor devices*, Wiley-Blackwell, 2007.